論文 / 著書情報
Article / Book Information

Title	Ultrafine nanoporous palladium-aluminum film fabricated by citric acid-assisted hot-water-treatment of aluminum-palladium alloy film
Authors	Takashi Harumoto,Yohei Tamura,Takashi Ishiguro
Citation	AIP Advances, Vol. 5, ,
発行日/Pub. date	2015, 1
公式ホームページ /Journal home page	http://scitation.aip.org/
権利情報/Copyright	Copyright (c) 2015 American Institute of Physics

AIP Advances

Ultrafine nanoporous palladium-aluminum film fabricated by citric acid-assisted hot-water-treatment of aluminum-palladium alloy film

Takashi Harumoto, Yohei Tamura, and Takashi Ishiguro

Citation: AIP Advances **5**, 017146 (2015); doi: 10.1063/1.4907049
View online: http://dx.doi.org/10.1063/1.4907049
View Table of Contents: http://scitation.aip.org/content/aip/journal/adva/5/1?ver=pdfcov
Published by the AIP Publishing

Ultrafine nanoporous palladium-aluminum film fabricated by citric acid-assisted hot-water-treatment of aluminum-palladium alloy film

Takashi Harumoto, Yohei Tamura, and Takashi Ishiguro[a]
Department of Materials Science and Technology, Tokyo University of Science, 6-3-1 Niijyuku, Katsushika-ku, Tokyo, 125-8585, Japan

(Received 3 December 2014; accepted 20 January 2015; published online 27 January 2015)

Hot-water-treatment has been adapted to fabricate ultrafine nanoporous palladium-aluminum film from aluminum-palladium alloy film. Using citric acid as a chelating agent, a precipitation of boehmite (aluminum oxide hydroxide, AlOOH) on the nanoporous palladium-aluminum film was suppressed. According to cross-sectional scanning transmission electron microscopy observations, the ligament/pore sizes of the prepared nanoporous film were considerably small (on the order of 10 nm). Since this fabrication method only requires aluminum alloy film and hot-water with chelating agent, the ultrafine nanoporous film can be prepared simply and environmentally friendly. [http://dx.doi.org/10.1063/1.4907049]

Nanoporous metals are applied to catalysts,[1] sensors[2] and supercapacitors,[3] since they exhibit large surface-area-to-volume ratios. The most usual fabrication method of nanoporous metals is dealloying, which is based on chemical or electrochemical dissolution process of the less noble metal from a precursor alloy. Raney nickel (Ni), which is fabricated from nickel-aluminum (Ni-Al) alloy using alkaline solution, is a famous example of dealloying and has been applied as a catalyst for hydrogenation.[4]

The ligament/pore sizes of nanoporous metals can be controlled by selecting composition of the precursor alloy,[5,6] microstructure of the precursor alloy,[7] dealloying solution,[8–10] dealloying temperature,[11] dealloying time,[12] etc. In literature, ultrafine nanoporous metals (ligament/pore sizes : ~ 10 nm), of which property may be different from bulk, could be achieved by dealloying at low temperature,[11,13] addition of surfactants to the dealloying solution[14,15] or addition of magnesium (Mg) to the precursor alloy.[6,10,16,17]

According to literatures and our previous study, a hot-water-treatment (temperature of the water: 368 K) of an Al film results in boehmite (aluminum oxide hydroxide, AlOOH) film.[18–21] It is assumed from the surface morphology that, during the hot-water-treatment, Al partially dissolves into water and precipitates as the hydroxide on the film. Thus, we expected that, similar to the case of addition of Mg, ultrafine nanoporous metal films could be synthesized using a combination of the hot-water-treatment and the Al alloy precursor film.

In this study, since nanostructured palladium (Pd) has various applications such as a catalyst,[22] a hydrogen storage medium[23,24] and a sensor for hydrogen,[25,26] we try to fabricate nanoporous palladium films by the hot-water-treatment of Al-Pd alloy film.

Al-Pd alloy films were prepared using a radio frequency (r.f.) magnetron sputtering apparatus. An Al disk (diameter: 3 inches, purity: 99.99 %) with Pd sectors (purity: 99.95 %) was adopted as a target and a target-to-substrate distance was adjusted to 44 mm. The pressure before gas introduction was better than 3×10^{-5} Pa and pure argon gas was filled at 1.1 Pa. The r.f. power of 60 W was applied to the target, and 70-nm-thick Al-Pd alloy film was deposited on Corning Eagle XG glass or nondoped silicon (Si) wafer with a native oxide at room temperature. The size and thickness of the

[a]Author to whom correspondence should be addressed. Electronic mail: ishiguro@rs.noda.tus.ac.jp.

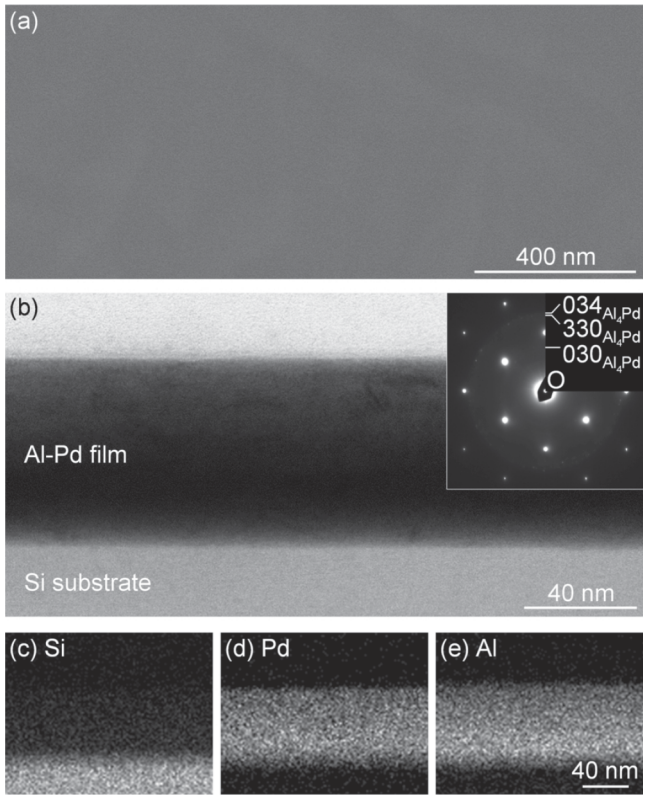

FIG. 1. (a) FE-SEM surface and (b) STEM-BF cross-sectional images of the as-deposited Al-Pd film. Inset figure of (b) is SAED pattern of the cross-section. (c), (d) and (e) are STEM-EDS elemental mapping images of (b).

substrates were 20 mm × 15 mm and 0.7 mm, respectively. After the film deposition, the film was hot-water-treated, *i.e.* the film was boiled in 1 L ultrapure water (resistivity: 18.2 MΩ·cm) at 368 K for 110 minutes. As a chelating agent for Al (the explanation for the addition of the chelating agent can be found later), a small amount of citric acid monohydrate (purity: 99.7 %; purchased from Wako pure chemical industries) was added to the ultrapure water.

The surface morphologies of the specimens were analyzed using field emission scanning electron microscope (FE-SEM) (S-4200; Hitachi high-technologies) operated at 5 kV. Scanning transmission electron microscope (STEM) (HD-2300C; Hitachi high-technologies) was also adopted to observe cross-sectional microstructure of the film. STEM was operated at 200 kV, and both bright-field (BF) and high-angle annular dark-field (HAADF) images were recorded. The elemental analysis of the cross-section was performed using an energy dispersive X-ray spectroscopy (EDS) (EDAX rTEM; Ametek). Selected area electron diffraction (SAED) patterns of the cross-section were acquired using conventional transmission electron microscope (TEM) (JEM-2000FX; JEOL) operated at 200 kV. The camera length was determined using spots of Si(100) wafer. The cross-sectional specimens were prepared using argon (Ar) ion milling (PIPS; Gatan).

The surface and cross-sectional views of the as-deposited Al-Pd film are shown in Fig. 1. According to the FE-SEM surface image (Fig. 1(a)), the surface is flat and no in-plane texture is observed. The cross-sectional STEM image reveals that the film is homogeneous and has no pore (Fig. 1(b)). The EDS elemental maps demonstrate that Al and Pd are uniformly distributed in the film (Figs. 1(c)-1(e)). The composition of the film determined by the EDS spectrum is 83 at%Al - 17 at%Pd, indicating that the as-deposited film is Al-rich. SAED pattern of the as-deposited film is shown in an inset of Fig. 1(b) and all observed rings are related to λ (Al_4Pd: 80 at%Al - 20 at%Pd) phase.[27–29] This result is in agreement with the EDS analysis from the view point of composition. Since the film consists of single λ phase, no segregation of elements occurs and the film is homogeneous. The lattice spacings calculated from the SAED pattern are almost equal to the bulk lattice

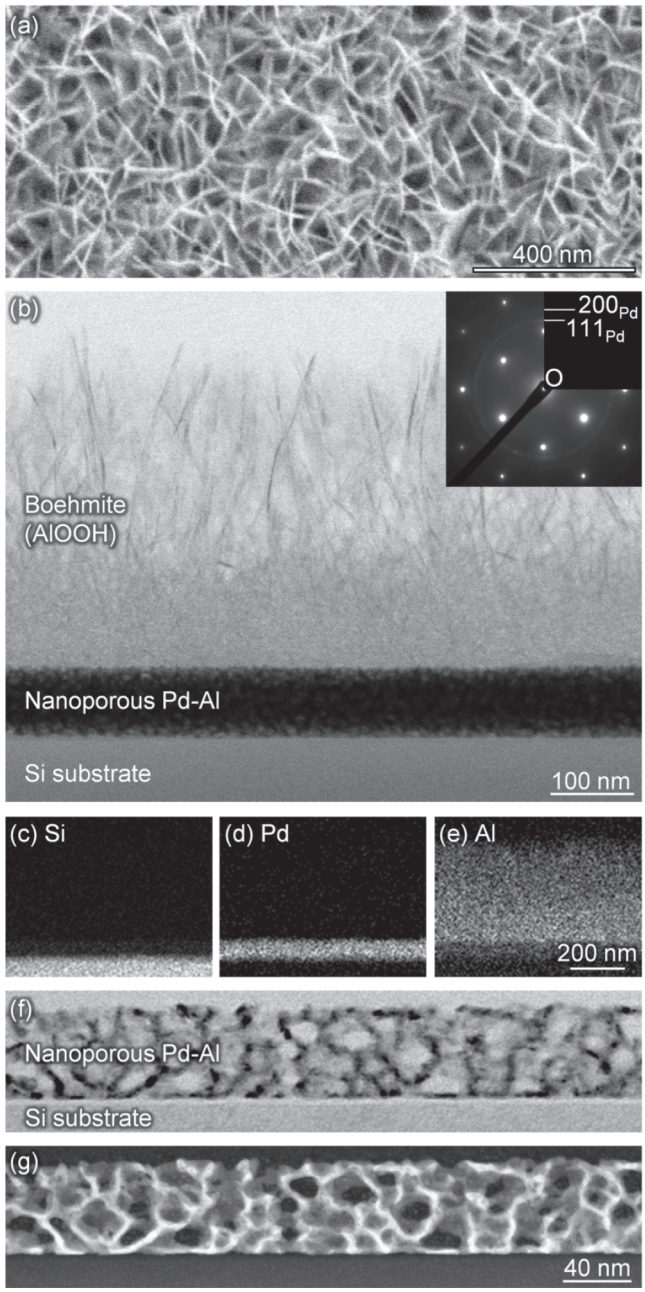

FIG. 2. (a) FE-SEM surface and (b) STEM-BF cross-sectional images of the hot-water-treated film. Inset figure of (b) is SAED pattern of the cross-section. (c), (d) and (e) are STEM-EDS elemental mapping images of (b). (f) and (g) are STEM-BF and corresponding STEM-HAADF images at the region where the nanoporous Pd-Al is observed clearly, although the boehmite layer has been ion-milled completely.

spacings of λ phase.[28] It should be noted that the bright spots correspond to single-crystal Si(100) water.

The hot-water-treatment of the Al-Pd film in ultrapure water results in the layered structure, which is composed of a boehmite (AlOOH) layer and a nanoporous Pd-Al layer (Figs. 2(b)-2(e)). Since the nanoporous Pd-Al is covered by the boehmite layer, it is not observed in the FE-SEM surface image (Fig. 2(a)). The surface of the boehmite layer is desert rose-like structure, which is in agreement with the case of pure Al film.[18–21] The thickness of the nanoporous Pd-Al is almost equal

to one of the as-deposited film while the composition of the nanoporous Pd-Al is 57 at%Al - 43 at%Pd. Thus, the selective dissolution of Al from the film occurs and the dissolved Al precipitates onto the film as boehmite. Under the assumption that no Pd dissolution occurs, it is estimated from the composition change that 73% of Al content in the film has been transformed into AlOOH and 27% of Al remains at the nanoporous layer. It should be noted that the boehmite layer consists of a dense underlayer and a sparse upper-layer, although we cannot explain how these two layers formed during the hot-water-treatment at this moment. SAED pattern of the hot-water-treated film is shown in an inset of Fig. 2(b) and consists of rings corresponding to face-centered cubic (fcc) Pd. The measured lattice spacings of fcc Pd are ~1.6% larger than the bulk value,[27] indicating Al incorporation into fcc Pd lattice. The close view of the nanoporous Pd-Al layer is shown Figs. 2(f) and 2(g). Since these images were acquired at the very thin region, where the specimen was fully milled by Ar-ions, no boehmite remains on the nanoporous layer. It is clearly observed that the nanoporous Pd-Al layer is composed from ultrafine ligaments and pores with the sizes of the order of 10 nm. As HAADF image corresponds mainly to charge density and not to diffraction contrast, the nanoporous structure is obviously observed than BF image. Although the details are under investigation, it is anticipated that the Pd-rich ligaments are formed during the hot-water-treatment, since the segregation of Pd was not confirmed at the as-deposited state.

To suppress the precipitation of boehmite and exposure the nanoporous Pd-Al to surface, citric acid was adopted as a chelating agent for Al ions. Fig. 3 shows photos and FE-SEM images of films hot-water-treated in a dilute aqueous solution of citric acid (concentration of citric acid: 1.0×10^{-6} to 1.0×10^{-3} mol/L). It is clear that the addition of the chelating agent suppress the formation of the boehmite layer (Figs. 3(b) and 3(c)), although a redundant addition leads to peeling of the nanoporous Pd-Al layer (Fig. 3(d)). In contrast, the insufficient addition results in the partial residues of the boehmite layer (Fig. 3(a)). Accordingly, the optimum amount of the citric acid is 1.0×10^{-4} to 1.0×10^{-5} mol, which is an enough amount for chelating Al in the as-deposited Al-Pd film (Al content in the as-deposited film: $\sim 1 \times 10^{-6}$ mol), in 1 L ultrapure water. The cross-sectional STEM image and EDS elemental mapping images of the film treated in 1.0×10^{-5} mol/L are shown in Fig. 4. The ultrafine nanoporous structure is observed and the ligament/pore sizes of the nanoporous film are the order of 10 nm (Figs. 4(a)-4(c)), which are comparable to the case of Mg addition.[6,10,16,17] The composition of the nanoporous film was 34 at%Al - 66 at%Pd, indicating that some amount of Al remains in nanoporous film (Figs. 4(e) and 4(f)). Under the

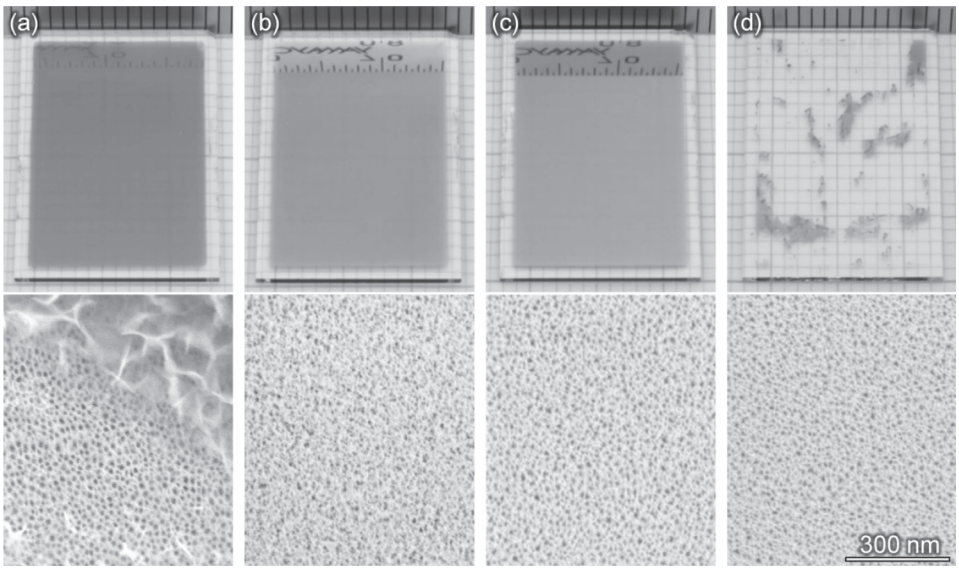

FIG. 3. Photos (upper) and FE-SEM surface images (lower) of the films hot-water-treated in the aqueous solution of citric acid. The concentrations of citric acid are (a) 1.0×10^{-6}, (b) 1.0×10^{-5}, (c) 1.0×10^{-4} and (d) 1.0×10^{-3} mol/L.

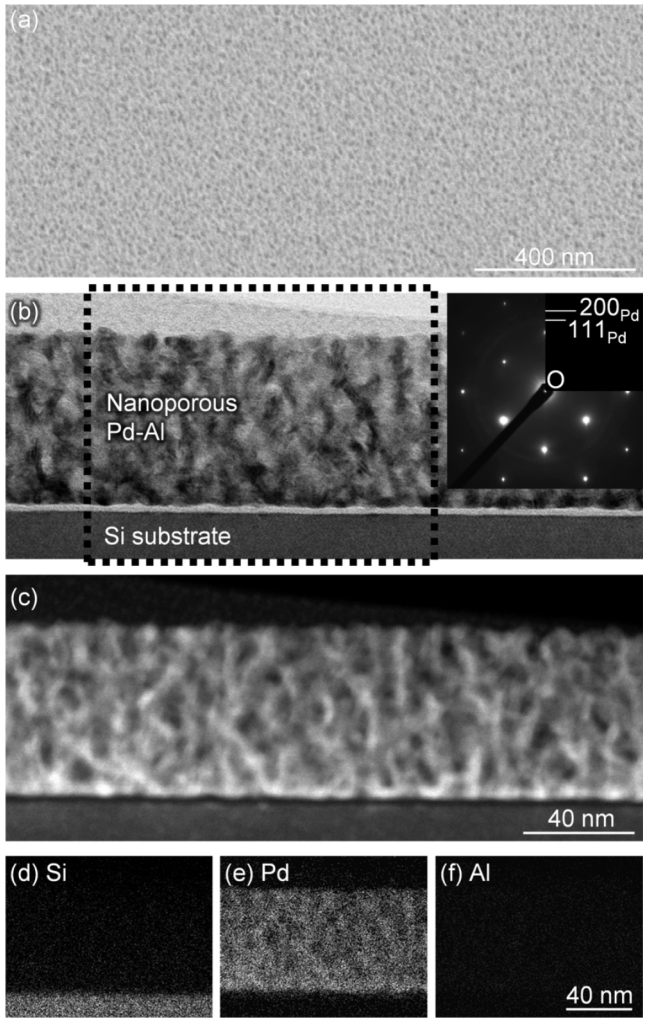

FIG. 4. (a) FE-SEM surface, (b) STEM-BF cross-sectional and (c) corresponding STEM-HAADF cross-sectional images of the film hot-water-treated in aqueous solution of citric acid (concentration of citric acid: 1.0×10^{-5} mol/L). Inset figure of (b) is SAED pattern of the cross-section. (d), (e) and (f) are STEM-EDS elemental mapping images of the region indicated by a dotted line rectangle in (b).

assumption that no Pd dissolution occurs, the composition difference from the as-deposited indicates that 89% of Al content in the film is dissolved. This could result in approximately 74% porosity. According to the SAED pattern (inset of Fig. 4(b)), the nanoporous film consists of fcc Pd. In comparison to the bulk values,[27] the lattice spacings of the nanoporous film are ~1.7% expanded and this relates to the Al incorporation. Thus, although the fabricated film is not pure Pd, the ultrafine nanoporous Pd-Al film can be fabricated by the citric acid-assisted hot-water-treatment of Al-Pd alloy film. Because no difficult procedure and no harmful chemicals are required, the fabrication method proposed here is simple and environmentally friendly approach. It should be noted that this method can be applied in the case of other noble metal-Al precursor films.

In conclusion, the simple preparation method based on the hot-water-treatment has been proposed to fabricate the nanoporous Pd-Al film from Al-Pd alloy film. Since the dissolved Al inclines to precipitate as boehmite, the addition of a small amount of chelating agent was required. According to cross-sectional STEM observations, the pore/ligament sizes of the prepared nanoporous film are on the order of 10 nm, which is comparable to films fabricated from Mg alloy film in literatures. It should be noted that the method proposed here is environmentally friendly, since harmful chemicals such as a strong acid are not employed.

ACKNOWLEDGMENTS

This research is partially supported by Grant-in-Aid for Scientific Research (No.: 25870772) from Japan Society for the Promotion of Science (JSPS).

[1] A. Wittstock, V. Zielasek, J. Biener, C. M. Friend, and M. Baumer, Science **327**, 319 (2010).
[2] J. Wang, D. F. Thomas, and A. Chen, Anal. Chem. **80**, 997 (2008).
[3] X. Y. Lang, A. Hirata, T. Fujita, and M. W. Chen, Nat. Nanotechnol. **6**, 232 (2011).
[4] M. Raney, U.S. patent 1,628,190 (10 May 1927).
[5] S. Supansomboon, A. Porkovich, A. Dowd, M. D. Arnold, and M. B. Cortie, ACS Appl. Mater. Interfaces **6**, 9411 (2014).
[6] L. Wang and T. J. Balk, Phil. Mag. Lett. **94**, 573 (2014).
[7] Q. Q. Kong, L. X. Lian, Y. Liu, and J. Zhang, Mater. Lett. **127**, 59 (2014).
[8] J. F. Huang and I. W. Sun, Adv. Funct. Mater. **15**, 989 (2005).
[9] N. A. Senior and R. C. Newman, Nanotechnology **17**, 2311 (2006).
[10] H. Ji, X. G. Wang, C. C. Zhao, C. Zhang, J. L. Xu, and Z. H. Zhang, CrystEngComm **13**, 2617 (2011).
[11] Z. Q. Li, X. Lu, and Z. X. Qin, Int. J. Electrochem. Sci. **8**, 3564 (2013).
[12] L. Y. Chen, J. S. Yu, T. Fujita, and M. W. Chen, Adv. Funct. Mater. **19**, 1221 (2009).
[13] L. H. Qian, X. Q. Yan, T. Fujita, A. Inoue, and M. W. Chen, Appl. Phys. Lett. **90**, 153120 (2007).
[14] W. C. Li and T. J. Balk, Scripta Mater. **62**, 167 (2010).
[15] J. Schoop and T. J. Balk, Metall. Mater. Trans. A **45A**, 2309 (2014).
[16] H. Ji, J. Frenzel, Z. Qi, X. G. Wang, C. C. Zhao, Z. H. Zhang, and G. Eggeler, CrystEngComm **12**, 4059 (2010).
[17] L. Wang, N. J. Briot, P. D. Swartzentruber, and T. J. Balk, Metall. Mater. Trans. A **45A**, 1 (2014).
[18] G. L. Dorer and V. Mikelsons, U.S. patent 4,190,321 (26 February 1980).
[19] T. Ishiguro, T. Hori, and Z. Y. Qiu, J. Appl. Phys. **106**, 023524 (2009).
[20] A. Egashira, T. Ube, Y. Hosoki, T. Harumoto, and T. Ishiguro, Mater. Trans. **54**, 1025 (2013).
[21] T. Ube, T. Harumoto, and T. Ishiguro, Jpn. J. Appl. Phys. **53**, 066701 (2014).
[22] S. W. Kim, M. Kim, W. Y. Lee, and T. Hyeon, J. Am. Chem. Soc. **124**, 7642 (2002).
[23] V. Berube, G. Radtke, M. Dresselhaus, and G. Chen, Int. J. Energ. Res. **31**, 637 (2007).
[24] P. J. Cappillino, K. M. Hattar, B. G. Clark, R. J. Hartnett, V. Stavila, M. A. Hekmaty, B. W. Jacobs, and D. B. Robinson, J. Mater. Chem. A **1**, 602 (2013).
[25] U. Schlecht, K. Balasubramanian, M. Burghard, and K. Kern, Appl. Surf. Sci. **253**, 8394 (2007).
[26] D. Luna-Moreno and D. Monzon-Hernandez, Appl. Surf. Sci. **253**, 8615 (2007).
[27] A.J. McAlister, Bull. Alloy Phase Diagrams **7**, 368 (1986).
[28] M. Yurechko, A. Fattah, T. Velikanova, and B. Grushko, J. Alloys Compds. **329**, 173 (2001).
[29] H. Okamoto, J. Phase Equilib. **24**, 196 (2003).